



STRUCTURAL PROPERTIES AND SURFACE MORPHOLOGY ANALYSIS OF NANOPHOTONIC LiNbO_3

Makram. A. Fakhri^{1,2}, Y. Al-Douri¹, Evan. T. Salim³, Uda. Hashim¹, Yushamdan Yusof⁴, Ee Bee Choo⁴, Zaid T. Salim¹ and Yaseen N. Jurn⁵

¹Institute of Nano Electronic Engineering, University Malaysia Perlis, Perlis, Malaysia

²Laser and Optoelectronic department, University of Technology, Baghdad, Iraq

³Laser science branch, University of Technology, Baghdad, Iraq

⁴School of Physics, USM, Penang, Malaysia

⁵School of Computer and Communication Engineering, University Malaysia Perlis, Perlis, Malaysia

E-Mail: mokaram_76@yahoo.com

ABSTRACT

Lithium niobate (LiNbO_3) nanostructures are prepared on n-silicon substrate by spin coating technique. The mixture was prepared with stirrer times; 8 h, 24 h and 48 h. They are characterized and analyzed by Atomic Force Microscopy (AFM) and X-ray diffraction (XRD). The measurements show that as stirrer time increases, the structures start to crystallize to become more regular distribution, which helps to use in optical waveguide and other optoelectronics

Keywords: lithium niobate, structural properties, Photonic device, optical waveguide, thin film preparation.

INTRODUCTION

Lithium Niobate (LN) is a very important optical material which is widely used by the Photonics industry, mainly due to its excellent electro/acousto-optical properties (E. Marenga and C.Aruta, 2009)(Makram A. Fakhri, Y. Al-Douri, 2015). Lithium niobate (LiNbO_3) is an important ferroelectric material because of its excellent piezoelectric, electrooptical, pyroelectrical and photo-refractive properties (M. Aufray and S. Manuel, 2009). It is a widely used as polar material for Photonic applications (Ch. Fan and B. Poumellec, 2012), in addition, its employed in nonlinear optics for frequency conversion and in telecommunication for electro-optic modulation (L. Cao and A. Aboketaf, 2014). It is a very attractive material for the fabrication of optical waveguide devices (J. Li, Dan-feng Lu, 2014). Recently for optical devices due to their mechanical robustness, good availability, optical homogeneity (P. Galinettoa and M. Marinonea, 2007), integrated optics with lasers, modulators (W-K. Kim and S-W. Kwon, 2009), and filters on a single LiNbO_3 wafer (J. Guo and J. Zhu, 2013) are especially promising. Thin films of nanophotonic LiNbO_3 have been studied for use in an integrated form with unique pyroelectric, piezoelectric (H. Chen and T. Lv, 2013), and nonlinear optical properties, which would make it an ideal material for the fabrication of surface acoustic wave (SAW) (H.K. Lam and J.Y. Dai, 2004), Optoelectronic and optical devices (T. Zhang and B. Wang, 2004), (Makram A. Fakhri, Y. Al-Douri, 2015).

LiNbO_3 Photonic crystal was prepared using various experimental techniques such as sputtering (V. Iyevlev and A. Kostyuchenko, 2011), liquid phase epitaxial (LPE) (Yi Lu and Peter Dekker, 2009), metal organic chemical vapor deposition (MOCVD) (Y. Akiyama and K. Shitanaka, 2007), soft- chemistry (M. Nyman and T. M Anderson, 2009), hydrothermal methods (R. Ageba and Y. Kadota, 2010), and pulsed laser deposition (PLD) (Y-J. Kang and S-Y. Jeong, 2006).

This paper reports on the production of LiNbO_3 nano and micro photonic crystal by utilizing the Pechini route (Sol-gel). The phase evolution with the molarities concentration was also studied by using XRD because it is the important part of our work and application on Optical waveguides from thin film nanoparticles LiNbO_3 nano and micro photonics

EXPERIMENTAL PROCESS

The preparation procedure for LiNbO_3 films by using Nb_2O_5 (ultra-purity, 99.99%), and citric acid (CA.) are used without further purification. The solution is prepared by mixing Li_2CO_3 , Nb_2O_5 , citric acid and Ethylene Glycol. The molar ratio between Li_2CO_3 and Nb_2O_5 was 1:1 in order to maximize the formation of LiNbO_3 stoichiometry phase. Firstly, the Li_2CO_3 , Nb_2O_5 , and citric acid were dissolved in Ethylene Glycol with heating and stirring at 90 °C for (8 h, 24 h, 48 h) hours, then mixed all together, with continued heating and stirring at the 90 °C for (8 h, 24 h, 48 h) hour. To obtain homogeneous and crack-free films of LiNbO_3 , the precursor was deposited by spin coating technique on silicon substrates at a spinning speed of 3000 rpm for 30 sec. Seven layers were prepared, the film was dried at 120 °C for 5 min and calcined at 250 °C for 30 min in static air and oxygen atmosphere to remove the organics then it was annealing at 500 °C.

RESULTS AND DISCUSSION

Structural properties

The XRD of LiNbO_3 nanostructures deposited on Si substrates grown by a sol-gel method is shown in Figure-1. The crystalline structure of LiNbO_3 nano and micro structures is found to have hexagonal structure. It is observed from Figure. 1 that the peaks at $2\theta = 23.634, 32.637, 34.674, 48.355, 53.106, \text{ and } 55.879$ correspond to (012), (104), (110), (024), (116) and (122)



planes. So, the crystalline structure will be more crystalline and more purity for LiNbO_3 with increasing the stirrer time as shown in Figure-1. The measured structural properties of LiNbO_3 nanostructures are listed in Table-1. Crystallite size (D) was calculated using Scherrer's formula (A.S. Ibraheam, Y. Al-Douri, 2015).

$$D = K \lambda / \beta \cos \theta \quad (1)$$

Where K is a constant taken to be 0.94, λ is the wavelength of X-ray used ($\lambda = 1.54 \text{ \AA}$), β is the full width at half maximum of XRD pattern and θ is Bragg's angle, around 26.41° .

In addition, the dislocation density (δ) and strain (ϵ) of LiNbO_3 nanostructures were determined using the following relations (Makram A. Fakhri, Y. Al-Douri, 2015).

$$\delta = 1 / D^2 \quad (2)$$

$$\epsilon = \beta / 4 \tan \theta \quad (3)$$

The interplanar distance (d) is calculated for all set of LiNbO_3 nanostructures using Bragg's formula (Makram A. Fakhri, Y. Al-Douri, 2015).

$$d = h \lambda / 2 \sin \theta \quad (4)$$

Where h is a different value because we have a hexagonal Crystal system then the lattice parameters a and c were calculated by using hexagonal Miller indices equation. Figure-1 shows the XRD pattern obtained from LiNbO_3 thin films deposited on N-type Si substrates. All the reflection peaks could be indexed to the hexagonal structure with lattice parameters $a = 5.145$, $c = 13.858$,

which were very close to the reported data in the A.Z. Simões *et al.* (A.Z. Simões and M.A. Zaghe, 2004). The thin film was a polycrystalline structure after annealing at 500°C for 2 h in static air, two phase of Lithium niobate could be recognized, it is Δ and δ phases. We find a preferred phase that's who Δ phase was observed. However. And in the performed phase have a preferred orientation that who 012. The XRD clearly indicates the presence of a small amount of secondary Li deficient phase (LiNb_3O_8) at all of molarities concentrations'. This phase is originated from an interface reaction between the Oxygen and LiNbO_3 then this phase could be detected by XRD is due to its high crystallization temperature and already this phase will be detected with increase the time of stirrer because the increased hours of mixing increases the possibility for total interaction between the chemicals and thus improves the purity of the final solvent mixture, and is found at peaks $2\theta = 24.407$ and 30.262 correspond to (400) and (410) planes at higher stirrer time, and more than one peak its 35.981 at (212) plane at lower stirrer time, this is attributed to annealing effect in static air and oxygen atmosphere and total interaction between the chemicals, There is no impurities like Nb_2O_5 , were detected in high stirrer time Because the increased hours of mixing increases the possibility for total interaction between the chemicals and thus improves the purity of the final solvent mixture, but in low of stirrer time we find in results a Nb_2O_5 is shown at peaks $2\theta = 24.433$ and 31.623 correspond to (-105) and (014) planes, the planes for using the Nb_2O_5 was shown as a raw material any way they not effect on our structure because it's a minority. The measured lattice constants have showed good accordance with experimental values as given in Table-1.

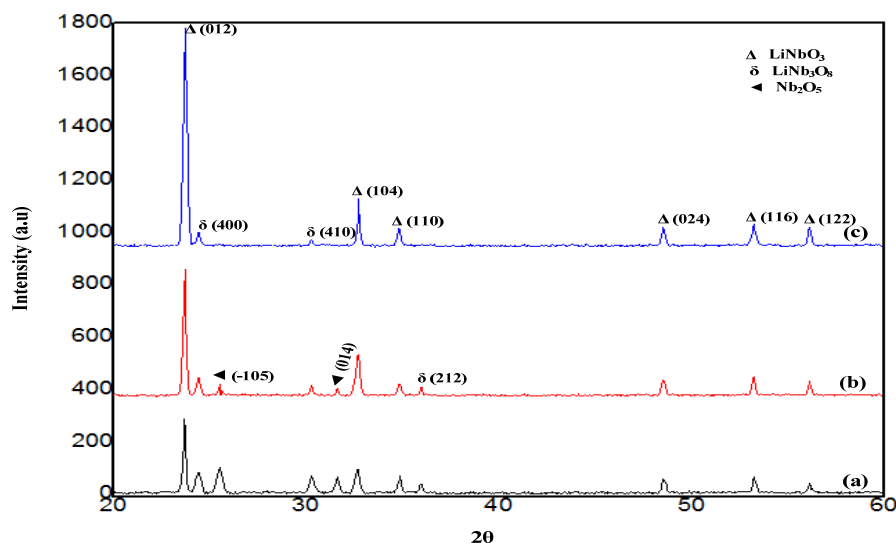


Figure-1. XRD patterns of LiNbO_3 nanostructures with different stirrer time. (a) 8 h, (b) 24 h, and (c) 48 h.

**Table-1.** Structural parameters of LiNbO₃ nanostructures at different stirrer times.

Stirrer time (h)	Orientation hkl	Peak (θ)	Particle size (nm)	Dislocation density (δ) (1014) (lines/m ²)	Strain (10 ⁻³)	d _{hkl} (Å)	Lattice constants (Å)	Roughness (nm)
8	012	23.738	92.6371	0.000117	0.835339	3.74508	a=5.1566 c=13.85	5.5
	104	33.031	47.2789	0.000447	0.839386	2.70961	a=5.1566 c=13.85	
	110	35.224	71.3362	0.000197	0.488195	2.54577	a=5.1566 c=13.85	
	024	47.517	59.4306	0.000283	0.31739	1.91194	a=5.1566 c=13.85	
	116	54.607	51.0116	0.000384	0.276939	1.67926	a=5.1566 c=13.85	
	122	58.312	38.9286	0.00066	0.316165	1.58108	a=5.1566 c=13.85	
24	012	23.713	55.5797	0.000324	0.83716	3.74898	a=5.1566 c=13.85	14.1
	104	33.037	56.7355	0.000311	0.41954	2.70916	a=5.1566 c=13.85	
	110	35.187	34.2378	0.000853	0.611616	2.54837	a=5.1566 c=13.85	
	024	47.493	44.5689	0.000503	0.254196	1.91284	a=5.1566 c=13.85	
	116	54.384	15.2881	0.004278	0.55919	1.68561	a=5.1566 c=13.85	
	122	56.544	23.1606	0.001864	0.34019	1.62625	a=5.1566 c=13.85	
48	012	23.690	18.5258	0.002914	0.838819	3.75254	a=5.1566 5.1561a 5.49340b c=13.85 13.8669a	20.9
	104	33.022	14.1833	0.004971	0.559917	2.71034	a=5.1566 c=13.85	
	110	35.181	19.0023	0.002769	0.375023	2.57366	a=5.1566 c=13.85	
	024	48.728	4.97597	0.040387	0.719699	1.86723	a=5.1566 c=13.85	
	116	54.347	4.36732	0.052429	0.653432	1.68668	a=5.1566 c=13.85	
	122	58.213	7.70544	0.016842	0.346083	1.63714	a=5.1566 c=13.85	

^aRef. (A.Z Simões, , A.H.M González, 2002) exp.; ^bRef. (I.-K. Jeong, 2011) exp

Morphological studies

The grain size and root mean square could be affected by molarity concentration. Figure-2 shows AFM images of the LiNbO₃ nanostructures with a uniform density surface and exhibits a decrease in grain size with increasing the stirrer time. The surface topography of LiNbO₃ nanostructures as observed from the AFM micrographs proves that the grains are uniformly distributed within the scanning area (5 μm x 5 μm), with individual columnar grains extending upwards. This surface characteristic is important from the topographic

images that found at 48 hours to be uniform, smooth and homogeneous than others.

In association with the increase of the average diameter of grain size from 18.53 to 92.64 nm, large grains appear on the proportion of solvent Figure-2(a). On the other hand, we note that the surface roughness increases with stirrer time because of the lack of solubility, so the roughness are ranging between 5.5-20.9nm.

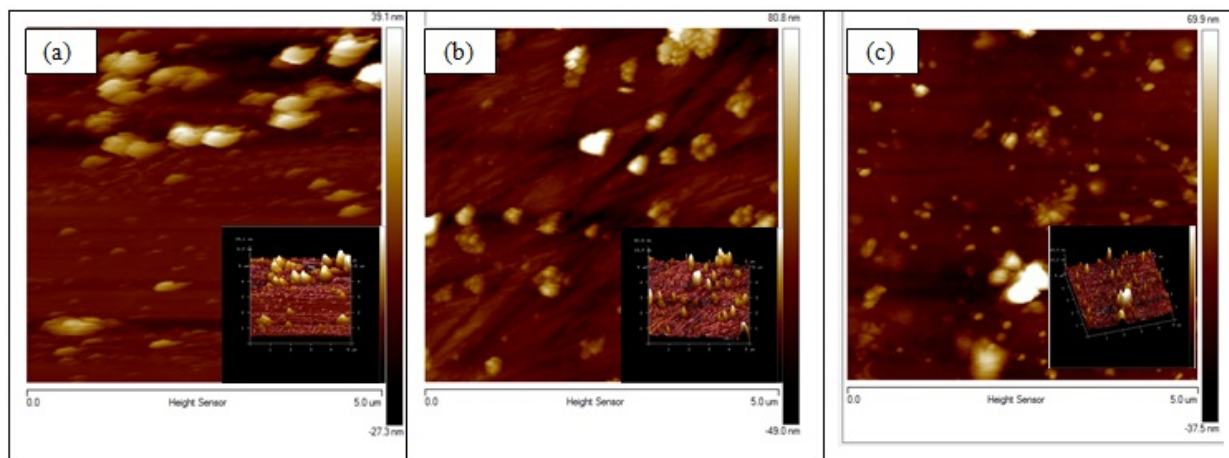


Figure-2. AFM images of LiNbO₃ nanostructures with different stirrer time. (a) 8 h , (b) 24 h, and (c) 48 h.

CONCLUSIONS

The LiNbO₃ nanostructures have been chemically prepared by spin-coating technique. SEM explains the samples will be smoother and better distribution with increasing the time of mixing. Based on XRD results, the LiNbO₃ nanostructures have polycrystalline in nature. The intensity is (780) peak showed at orientation (012) at $2\theta = 23.634^\circ$, a significant increasing as the spin coating speed at 3000 rpm. As expected, the structure is more crystalline as the time of stirrer increases. Also, AFM shows diameter of gain size (from 19.6 to 95.3) nm, and roughness ranging between 5-20 nm. Then from this results can used the optimum conditions (48 h) stirring time for the optical waveguide application.

REFERENCES

- [1] Ageba, R, Kadota, Y, Maeda, T, Takiguchi, N and Morita, T. (2010). Ultrasonically-assisted Hydrothermal Method for Ferroelectric Material Synthesis. *Journal of the Korean Physical Society*, 57, PP. 918-923.
- [2] Akiyama, Y, Shitanaka, K, Murakami, H, Shin, Y, Yoshida, M, Imaishi, N. (2007). Epitaxial growth of lithium niobate film using metal organic chemical vapor deposition. *Thin Solid Films*, 515, PP. 4975-4979.
- [3] Aufray, M, Menuel, S, Fort, Y, Eschbach, J, Rouxel, D, Vincent, B. (2009). New Synthesis of Nanosized Niobium Oxides and Lithium Niobate Particles and Their Characterization by XPS Analysis. *Journal of Nanoscience and Nanotechnology*, 19, PP. 4780-4785.
- [4] Cao, L, Aboketaf, A, Wang, Z, Preble, S. (2014). Hybrid amorphous silicon (a-Si:H)-LiNbO₃ electro-optic modulator. *Optics Communications*, 330 (1), PP. 40-44.
- [5] Chen, H, Lv, T, Zheng, A, Han, Y. (2013). Discrete diffraction based on electro-optic effect in periodically poled lithium niobate. *Optics Communications*, 294, PP. 202-207.
- [6] Fakhri, M. A, Al-Douri, Y, Hashim, U, Salim, E. T. (2015). Optical investigation of nanophotonic lithium niobate-based optical waveguide. *Applied physics B, Lasers and Optics*.
- [7] Fakhri, M. A, Al-Douri, Y, Hashim, U, Salim, E. T. (2015). Optical investigations of Photonics Lithium Niobate. *Solar Energy*, 120, PP. 381-388.
- [8] Fakhri, M. A, Al-Douri, Y, Hashim, U, Salim, E. T. (2015). Annealing Temperature Effects on Morphological and Optical Studies of Nano and Micro Photonics Lithium Niobate using for Optical Waveguide Applications. *Australian Journal of Basic and Applied Sciences*, 9(12), PP. 128-133.
- [9] Fan, C, Poumellec, B, Lancry, M, He, X, Zeng, H, Erraji-Chahid, A, Liu, Q, and Chen, G. (2012). Three-dimensional photoprecipitation of oriented LiNbO₃-like crystals in silica-based glass with femtosecond laser irradiation. *Optics Letters*, 37, PP. 2955-2957.
- [10] Galinetto, P, Marinone, M, Grando, D, Samoggia, G, Caccavale, F, Morbiato, A, Musolino, M. (2007). Micro-Raman analysis on LiNbO₃ substrates and surfaces: compositional homogeneity and effects of etching and polishing processes on structural properties. *Optics and Lasers in Engineering*, 45, PP. 380-384.
- [11] Guo, J, Zhu, J, Zhou, W, Huang, X. (2013). A plasmonic electro-optical variable optical attenuator based on side-coupled metal-dielectric-metal structure. *Optics Communications*, 294, PP. 405-408.



- [12] Ibraheam, A. S., Al-Douri, Y., Hashim, U., Ghezzer, M. R., Addou, A., Ahmed, W. K. (2015). Cadmium effect on optical properties of $\text{Cu}_2\text{Zn}_{1-x}\text{Cd}_x\text{SnS}_4$ quaternary alloys nanostructures. *Solar Energy*, 114, PP. 39–50.
- [13] Iyevlev, V. and Kostyuchenko, A. (2011). Electrical and structural properties of LiNbO_3 films, grown by RF magnetron sputtering. *Journal of Materials Science: Materials in Electronics*, 22, PP. 1258–1263.
- [14] Jeong, I.-K. (2011). Correlated Thermal Motion in Ferroelectric LiNbO_3 Studied Using Neutron Total Scattering and a Rietveld Analysis. *Journal of the Korean Physical Society*, 59, PP. 2756–2759.
- [15] Kang, Y., Jeong, S., Lee, S., Hwang, J., Kim, J., Cho, C. (2006). Hetero-Epitaxial Growth of LiNbO_3 Thin Film on $\text{GaN}/\text{Al}_2\text{O}_3$ by Pulsed Laser Deposition. *Journal of the Korean Physical Society*, 49, PP. S625–S628.
- [16] Kim, W., Kwon, S., Jeong, W., Son, G., Lee, K., Choi, W., Yang, W., Lee, H. and Lee, H. (2009). Integrated optical modulator for signal up conversion over radio-on-fiber link. *Optics Express*, 17, PP. 2638–2645.
- [17] Lam, H. K., Dai, J. Y., Chan, H. L. W. (2004). Orientation controllable deposition of LiNbO_3 films on sapphire and diamond substrates for surface acoustic wave device application. *Journal of Crystal Growth*, 268, PP. 144–148.
- [18] Li, J., Lu, D., and Qi, Z. (2014). Miniature Fourier transform spectrometer based on wavelength dependence of half-wave voltage of a LiNbO_3 waveguide interferometer. *Optics Letters*, 39, PP. 3923–3926.
- [19] Lu, Y. and Dekker, P. (2009). Growth and characterization of lithium niobate planar waveguides by liquid phase epitaxy. *Journal of Crystal Growth*, 311, PP. 1441–1445.
- [20] Marenga, E., Aruta, C., Fanelli, E., Barra, M., Pernice, P., Aronne, A. (2009). Sol-gel synthesis of nanocomposite materials based on lithium niobate nanocrystals dispersed in a silica glass matrix. *Journal of Solid State Chemistry*, 182, PP. 1229–1234.
- [21] Nyman, M., Anderson, T. M. and Provencio, P. P. (2009). Comparison of Aqueous and Non-aqueous Soft-Chemical
- [22] Simoesa, A. Z., Zagheeta, M. A., Stojanovica, B. D., Gonzalez, A. H., Riccardia, C. S., Cantonic, M., Varela, J. A. (2004). Influence of oxygen atmosphere on crystallization and properties of LiNbO_3 thin films. *Journal of the European Ceramic Society*, 24, PP. 1607–1613.
- [23] Simões, A. Z., González, A. H. M., Cavaleiro, A. A., Zagheeta, M. A., Stojanovic, B. D., Varela, J. A. (2002). Effect of magnesium on structure and properties of LiNbO_3 prepared from polymeric precursors. *Ceramics International*, 28, PP. 265–270.
- [24] Syntheses of Lithium Niobate and Lithium Tantalate Powders. *Cryst. Growth Des*, 9, PP. 1036–1040.
- [25] Zhang, T., Wang, B., Zhao, Y., Fang, S., Ma, D., Xu, Y. (2004). Optical homogeneity and second harmonic generation in Li-rich Mg-doped LiNbO_3 crystals. *Materials Chemistry and Physics*, 88, PP. 97–101.